AIP Applied Physics Letters

Generation of self-healing and transverse accelerating optical vortices

Bing-Yan Wei, Peng Chen, Shi-Jun Ge, Wei Duan, Wei Hu, and Yan-Qing Lu

Citation: Applied Physics Letters **109**, 121105 (2016); doi: 10.1063/1.4963061
View online: http://dx.doi.org/10.1063/1.4963061
View Table of Contents: http://scitation.aip.org/content/aip/journal/apl/109/12?ver=pdfcov
Published by the AIP Publishing

APPLIED PHYSICS LETTERS **109**, 121105 (2016)

Generation of self-healing and transverse accelerating optical vortices

Bing-Yan Wei, Peng Chen, Shi-Jun Ge, Wei Duan, Wei Hu,[a)] and Yan-Qing Lu[b)]
National Laboratory of Solid State Microstructures, Collaborative Innovation Center of Advanced Microstructures and College of Engineering and Applied Sciences, Nanjing University, Nanjing 210093, China

(Received 20 June 2016; accepted 7 September 2016; published online 19 September 2016)

Self-healing and transverse accelerating optical vortices are generated via modulating Gaussian beams through subsequent liquid crystal q-plate and polarization Airy mask. We analyze the propagation dynamics of these vortex Airy beams, and find that they possess the features of both optical vortices and Airy beams. Topological charges and characteristics of nondiffraction, self-healing, and transverse acceleration are experimentally verified. In addition, vortex Airy beams with both topological charge and radial index are demonstrated and mode switch among Gaussian, vortex, vector, Airy beams and their combinations can be acquired easily. Our design provides a flexible and highly efficient way to generate unique optical vortices with self-healing and transverse acceleration properties, and facilitates prospective applications in optics and photonics. *Published by AIP Publishing.*
[http://dx.doi.org/10.1063/1.4963061]

Optical vortices (OVs) have been attracting intensive attention over the past few decades. Thanks to their helical wavefronts and donut-like intensity distributions,[1] OVs play important roles in optical tweezers,[2] opticial communications,[3] quantum computing,[4] high resolution imaging,[5] and so on. Recently, introducing more features to OVs has drawn particular interests. Nondiffraction property was introduced via specific high order Bessel beams[6] or by superposition of several OVs.[7] By imposing OVs on Airy beams (ABs), vortex Airy beams (VABs) possessing transverse acceleration property were proposed.[8] Additionally, ABs are also nondiffracting and hold self-healing feature.[9] Thus, VABs may bring a series of innovative characteristics to OVs and opportunities to corresponding applications.

Up to date, a few works were reported on the demonstration of VABs. A straightforward way is encoding a phase singularity into a cubic[10] or 3/2[11] phase pattern implemented by a spatial light modulator (SLM). However, beam expansion is required to match the size of SLM chip, which is composed of numerous discrete pixels driven separately.[12] The strategy suffers from high cost, optical inefficiency (less than 40%), and limited beam quality. The other is through illuminating a dielectric metasurface with an AB, which is also generated via an SLM.[13] The metasurface is fabricated through a time consuming femtosecond laser writing process, and the obtained geometric phase functions efficiently only for a fixed wavelength. Besides, the previous researches mainly focus on the transverse acceleration property and most of them are simulation works. Therefore, exploiting simple and efficient techniques for VABs generation and systematically investigating their propagation dynamics are of obvious significance.

Here, VABs are generated via modulating Gaussian beams through subsequent liquid crystal (LC) q-plate[14] and polarization Airy mask (PAM).[15] Both the LC geometric phase elements are made based on photoalignment technique with each exposure process costing only 5 min.[16] The optical setup is compact and the total efficiency is drastically improved to over 80%. We experimentally investigate the propagation dynamics of generated beams and verify the topological charge, quasi-nondiffraction, self-healing, and transverse acceleration properties of VABs. The work may enhance the applications of OVs in multi-dimensional particles manipulation, precise optical processing, lossless quantum-communication transmission, and even some uncharted fields.

The optical setup for the generation and measurement of VABs is schematically depicted in Fig. 1. A 671 nm Gaussian laser beam is adopted as the source. A polarizer and $\lambda/4$ plate are utilized to adjust the polarization state. The angle between the c-axis of the $\lambda/4$ plate and the polarizer direction is set to be 45° or −45° to get left or right circularly polarized light. Then the beam is converted to designed OV via specific q-plate. Finally, the VAB is generated after the modulation of LC PAM and a spherical lens ($f = 125$ mm). The resultant intensity distribution is captured by a CCD.

For q-plates, the direction of optical axis can be described as $\alpha(r, \varphi) = q\varphi + \alpha_0$, where (r, φ) is the polar coordinate representation, q is the topological charge of the q-plate, and α_0 is the initial angle when $\varphi = 0$.[17] For the LC PAM, its geometric

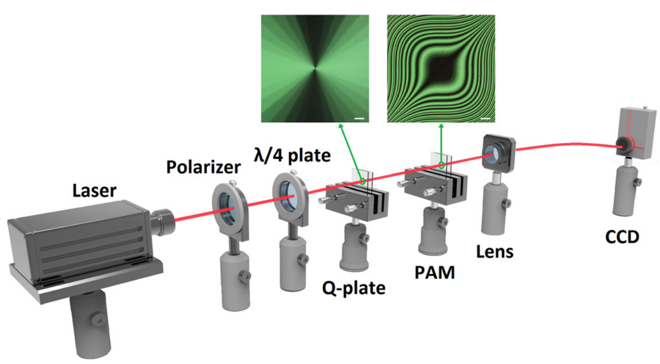

FIG. 1. The schematic optical setup for generating and measuring the VABs. The scale bar is 100 μm.

[a)]Electronic mail: huwei@nju.edu.cn
[b)]Electronic mail: yqlu@nju.edu.cn

phase distribution follows $\beta(x, y) = x^3 + y^3$ in the x-y plane. Both the two elements are fabricated as reported in our previous works.[14,15,18] Corresponding micrographs are shown in the upper row of Fig. 1. In our work, the phase retardations of the LC elements are electrically tuned to satisfy the half-wave condition. For a left circularly polarized input light, its electric-field can be described by Jones vector $\mathbf{E}_{\mathrm{in}} = E_0 \times [1, i]^{\mathrm{T}}$. After passing through the q-plate, it will be transformed into the following expression:[17]

$$\mathbf{E}_{\mathrm{out1}} = E_0 e^{i2q\varphi} e^{i2\alpha_0} \begin{pmatrix} 1 \\ -i \end{pmatrix}. \quad (1)$$

The emerging wave is right circularly polarized and transformed into a helical wave with orbital helicity $m = 2q$. After further propagating through the PAM, its Jones matrix M is multiplied; thus, the phase factor will be modulated as[15,19]

$$e^{i2q\varphi} e^{i2\alpha_0} M\left(\frac{x^3 + y^3}{2}\right)\begin{pmatrix} 1 \\ -i \end{pmatrix} = e^{i2q\varphi} e^{i2\alpha_0} e^{-i\left(x^3+y^3\right)} \begin{pmatrix} 1 \\ i \end{pmatrix}. \quad (2)$$

Obviously, the beam carries orbital angular momentum (OAM) given by $2q\hbar$, exhibits the characteristics of a cubic phase modulation, and keeps the original polarization state.

Figure 2(a) exhibits the intensity distribution of obtained VAB with designed topological charge $m = 2q = 1$. It consists of a ring-like main lobe and a family of side beamlets whose intensity decays exponentially. Theoretically, the incident light can be totally converted into the designed VAB, while an efficiency of 80% is obtained due to the reflection loss. To verify the topological charge, the astigmatic transformation method[20] is employed by substituting a cylindrical lens ($f = 100$ mm) for the spherical lens. Figure 2(b) shows the converted pattern captured at the Fourier transform plane. Obviously, the number of the dark stripes between the main transformed lobe is one, consistent with its topological charge. An $m = 2$ VAB is demonstrated as well, and its intensity distribution and the astigmatic transformation pattern are shown in Figs. 2(c) and 2(d), respectively. Thanks to the excellent flexibility of photoalignment technique, more complex OVs can be easily generated.[14] For instance, two high-order Laguerre–Gaussian (LG) beams with both topological charge and radial index (LG_1^1 and LG_1^2) are produced, and corresponding two-ringed OVs are shown in Figs. 2(e) and 2(f), respectively. They may find special applications in gravitational wave detection[21] and the trapping of cold atoms.[22] It is worth mentioning that mode switches among Gaussian, vortex, vector, Abs, and their combinations can also be realized. Briefly, by electrically tuning the phase retardation of LC PAM or q-plate it can be concluded that if they are equal to 0 or 2π simultaneously, Gaussian beam maintains, or if they are tuned separately, OV or AB will be generated accordingly. On the other hand, by rotating the $\lambda/4$ plate to obtain linear polarization, the previously generated OV or VAB will be changed to vector beam or vector Airy beam. This flexibility drastically facilitates the beam shaping and control.

We take $m = 1$ VAB as an example to measure the propagation dynamics. First, nondiffraction property is tested.

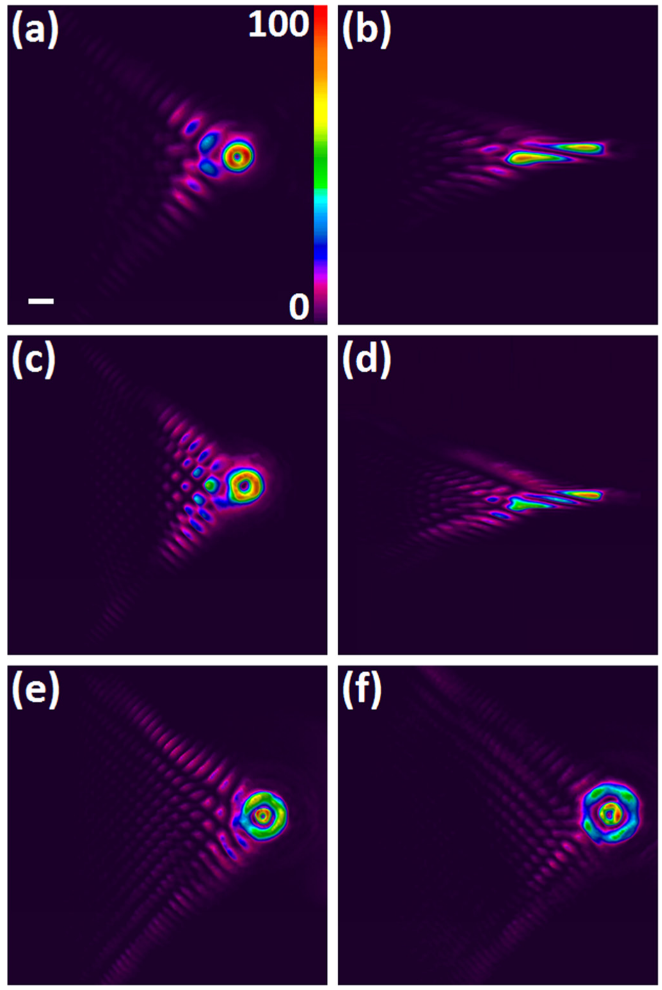

FIG. 2. Intensity distributions of (a) $m = 1$, (c) $m = 2$ VAB, and (b), (d) corresponding astigmatic transformation patterns. Intensity distributions of (e) LG_1^1 and (f) LG_1^2 VAB. The scale bar for all images is 500 μm.

Figures 3(a) and 3(b) depict the intensity profiles of OV nested in AB and in free space tested at the same distances, respectively. Herein, we define the focal plane of the spherical lens as the original recording point ($d = 0$ cm), and free space OV with the same full width at half maximum (FWHM) as $d = 0$ cm OV nested in AB is selected as a reference. For better comparison, the tendencies of intensity and FWHM changes versus d are calculated and presented in Figs. 3(c) and 3(d). Obviously, for OV in AB, the light intensities decrease and the FWHMs increase slower along propagation than OV in free space. Theoretically, for an ideal AB, which is infinite in space and energy, the beam profile is unaltered in propagation. Actually, produced ABs and VABs are finite; thus, only quasi-nondiffraction phenomenon can be observed.

Subsequently, the self-healing feature is investigated. A needle with a diameter of ~400 μm is inserted into the light path to partly block the main lobe and the distorted light fields along propagation are shown in Figs. 3(e)–3(g). At first, the main lobe is seriously destroyed, and then the broken OV recovers gradually with the VAB propagation. Astigmatic transformation is implemented again to verify the recovered topological charge, and the converted pattern is displayed in Fig. 3(h). A dark stripe can be clearly observed at the converted main lobe pattern in spite of some

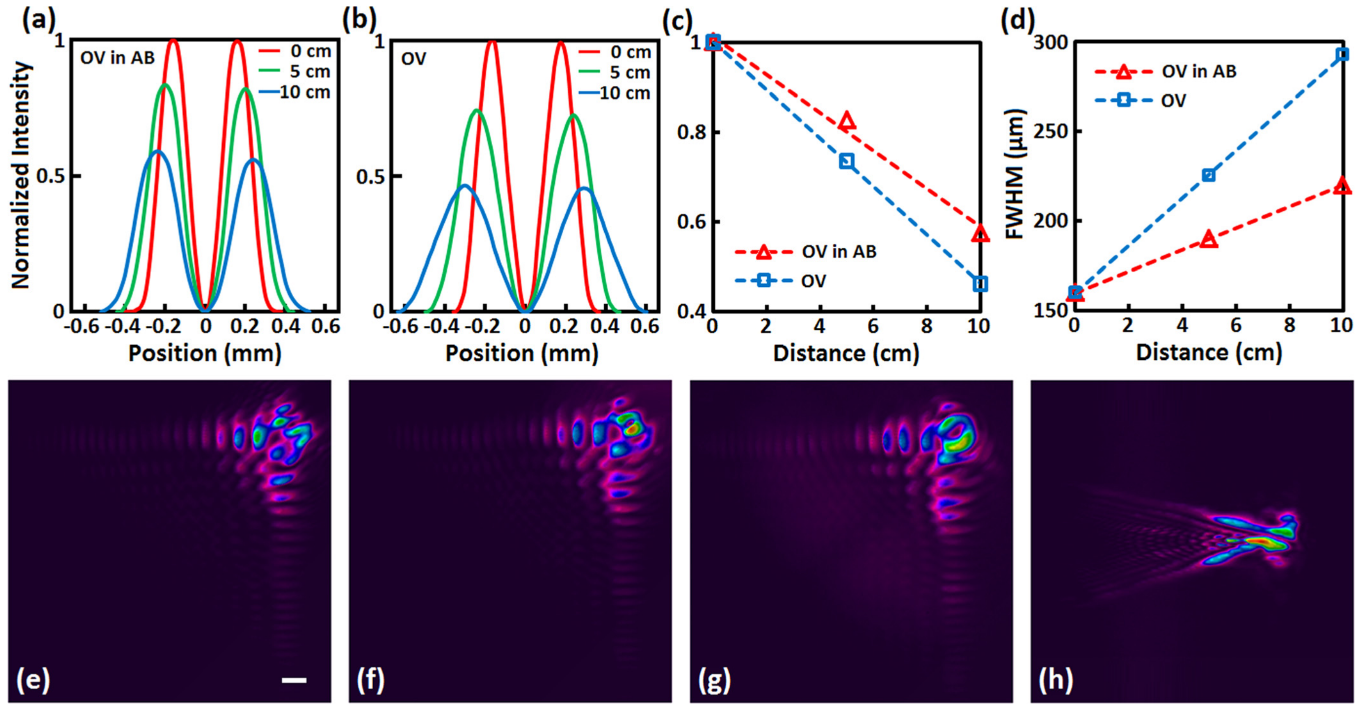

FIG. 3. Intensity profiles of OVs (a) nested in AB and (b) in free space recorded at the propagation distance 0 cm, 5 cm, and 10 cm, respectively. The dependencies of (c) normalized intensity and (d) FWHM on propagation distance. Intensity distributions at destroying point (e) $d = 0$ cm, and propagation distances: (f) $d = 6$ cm and (g) $d = 12$ cm; (h) astigmatic transformation pattern of (g). The scale bar for all images is 500 μm.

deformation, revealing a recovered $m = 1$ OV. The results vividly validate the self-healing property of the VAB. Finally, self-acceleration, another exotic characteristic of VAB, is studied. The transverse deflections at different propagation distances are measured and marked in Fig. 4 with three transverse profiles inserted. The red line is a parabolic fit of the experimental data, demonstrating the self-acceleration of OVs embedded in ABs.

In conclusion, we propose a simple and highly efficient way to generate high-quality VABs with excellent flexibility. Characteristics including topological charge and transverse acceleration are verified, and the self-healing and quasi-nondiffraction phenomena are experimentally demonstrated and analyzed. The technique also exhibits merits of low cost, compact configuration, electrical tunability, and switchability. The work supplies more possibilities in applications such as complex optical manipulation, precise optical processing, and so on.

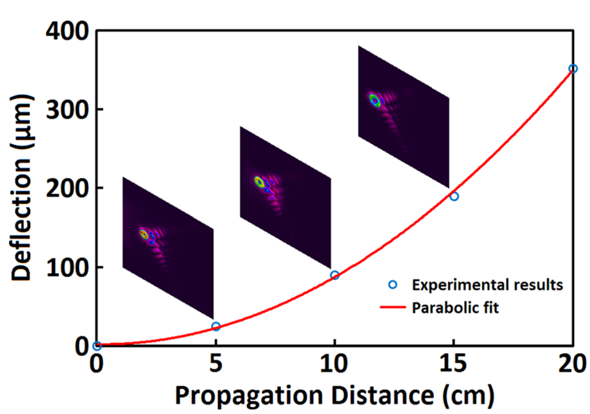

FIG. 4. Transverse acceleration of VAB as a function of propagation distance.

This work was sponsored by the NSFC programs (Nos. 11304151, 61490714, 61435008, and 61575093) and Jiangsu Province Innovation for PHD Candidate (No. KYLX16_0047).

[1]A. M. Yao and M. J. Padgett, Adv. Opt. Photonics **3**, 161 (2011).
[2]L. Paterson, M. P. MacDonald, J. Arlt, W. Sibbett, P. E. Bryant, and K. Dholakia, Science **292**, 912 (2001); X. L. Wang, J. Chen, Y. Li, J. Ding, C. S. Guo, and H. T. Wang, Phys. Rev. Lett. **105**, 253602 (2010); M. Gecevičius, R. Drevinskas, M. Beresna, and P. G. Kazansky, Appl. Phys. Lett. **104**, 231110 (2014).
[3]V. D'Ambrosio, E. Nagali, S. P. Walborn, L. Aolita, S. Slussarenko, L. Marrucci, and F. Sciarrino, Nat. Commun. **3**, 961 (2012); X. L. Wang, X. D. Cai, Z. E. Su, M. C. Chen, D. Wu, L. Li, N. L. Liu, C. Y. Lu, and J. W. Pan, Nature **518**, 516 (2015).
[4]G. Molina-Terriza, J. P. Torres, and L. Torner, Nat. Phys. **3**, 305 (2007).
[5]L. Yan, P. Gregg, E. Karimi, A. Rubano, L. Marrucci, R. Boyd, and S. Ramachandran, Optica **2**, 900 (2015); C. Zhang, C. Min, L. Du, and X. C. Yuan, Appl. Phys. Lett. **108**, 201601 (2016).
[6]A. Žukauskas, M. Malinauskas, and E. Brasselet, Appl. Phys. Lett. **103**, 181122 (2013); J. C. Gutiérrez-Vega and C. López-Mariscal, J. Opt. A: Pure Appl. Opt. **10**, 015009 (2008).
[7]Z. Bouchal and J. Courtial, J. Opt. A: Pure Appl. Opt. **6**, S184 (2004).
[8]H. T. Dai, Y. J. Liu, D. Luo, and X. W. Sun, Opt. Lett. **35**, 4075 (2010).
[9]G. A. Siviloglou, J. Broky, A. Dogariu, and D. N. Christodoulides, Phys. Rev. Lett. **99**, 213901 (2007); J. Broky, G. A. Siviloglou, A. Dogariu, and D. N. Christodoulides, Opt. Express **16**, 12880 (2008).
[10]M. Mazilu, J. Baumgartl, T. Čižmár, and K. Dholakia, Proc. SPIE **7430**, 74300C (2009); B. K. Singh, R. Remez, Y. Tsur, and A. Arie, Opt. Lett. **40**, 5411 (2015).
[11]H. T. Dai, Y. J. Liu, D. Luo, and X. W. Sun, Opt. Lett. **36**, 1617 (2011).
[12]Z. Zhang, Z. You, and D. Chu, Light: Sci. Appl. **3**, e213 (2014).
[13]J. Zhou, Y. Liu, Y. Ke, H. Luo, and S. Wen, Opt. Lett. **40**, 3193 (2015).
[14]W. Ji, C. H. Lee, P. Chen, W. Hu, Y. Ming, L. Zhang, T. H. Lin, V. Chigrinov, and Y. Q. Lu, Sci. Rep. **6**, 25528 (2016).
[15]B. Y. Wei, P. Chen, W. Hu, W. Ji, L. Y. Zheng, S. J. Ge, Y. Ming, V. Chigrinov, and Y. Q. Lu, Sci. Rep. **5**, 17484 (2015).
[16]V. Chigrinov, S. Pikin, A. Verevochnikov, V. Kozenkov, M. Khazimullin, J. Ho, D. D. Huang, and H. S. Kwok, Phys. Rev. E **69**, 061713 (2004); P. Chen, B. Y. Wei, W. Ji, S. J. Ge, W. Hu, F. Xu, V. Chigrinov, and Y. Q. Lu, Photonics Res. **3**, 133 (2015).

[17]L. Marrucci, C. Manzo, and D. Paparo, Phys. Rev. Lett. **96**, 163905 (2006).
[18]P. Chen, W. Ji, B. Y. Wei, W. Hu, V. Chigrinov, and Y. Q. Lu, Appl. Phys. Lett. **107**, 241102 (2015).
[19]M. Gecevičius, M. Beresna, R. Drevinskas, and P. G. Kazansky, Opt. Lett. **39**, 6791 (2014).
[20]V. Denisenko, V. Shvedov, A. S. Desyatnikov, D. N. Neshev, W. Krolikowski, A. Volyar, M. Soskin, and Y. S. Kivshar, Opt. Express **17**, 23374 (2009).
[21]M. Granata, C. Buy, R. Ward, and M. Barsuglia, Phys. Rev. Lett. **105**, 231102 (2010).
[22]M. A. Clifford, J. Arlt, J. Courtial, and K. Dholakia, Opt. Commun. **156**, 300 (1998).